RESEARCH PAPER

Fabrication and Evaluation of In Vitro Studies of Biodegradable and Antibacterial Composite Scaffolds Based on Polylactic Acid-Polycaprolactone-Hydroxyapatite Reinforced with Graphene and Zinc Oxide Nanoparticles for Use in Orthopedic Surgery

Farnaz Dehghani Firoozabadi [1], Ahmad Ramazani Saadatabadi [*,2], Azadeh Asefnejad [3]

* *ramazani@sharif.edu*

[1] **Biomedical Engineering (Biomaterials) Department, Islamic Azad University - Science and Research Branch, Tehran, Iran**

[2]* **Department of Chemical and Petroleum Engineering, Sharif University of Technology, Tehran, Iran**

[3] **Biomedical Engineering (Biomaterials) Department, Islamic Azad University - Science and Research Branch, Tehran, Iran**

Received: April 2022 Revised: June 2022 Accepted: June 2022

DOI: 10.22068/ijmse.2788

Abstract:

Introduction*: Fabrication of fully optimized tissue-engineered materials in order to simulating the natural structure, and enhancing the biological properties of damaged tissue is one of the major challenges in biomedical engineering and regeneration medicine. Although polymeric based membranes have revealed noticeable advancements in bone regeneration, their mechanical stiffens, electrical conductivity and bioactivity need to be tolerated.*

Methods*: Therefore, the present study is designed to generate a multifunctional biomaterial based on polylactic acid (PLA)/ polycaprolactone (PCL)/hydroxyapatite (HA) nanocomposite containing zinc oxide (ZnO) and Graphene (Gr) nanoparticles employing solvent casting combined with die cast techniques for using as absorbable joint implants in bone tissue regeneration. The physical, chemical, mechanical and biological properties of the produced nanocomposite biomaterials were analyzed in vitro. A detailed experimental evaluation between the nanocomposite coatings was carried out to shed light on the effect of ZnO and Gr nanoparticles on the properties.*

Results*: It was found that the nanocomposite contained 1% ZnO and 1% graphene with a Young's modulus of 1540.5 ± 169.426MPa and the pure sample had a Young's modulus of 1194.81±215.342MPa. The rate of elongation at break of the nanostructure contained 1% graphene was 5.1±0.816%. This value was 3.8±0.944% for the pure sample. The improvement in elongation at break is due to the presence of polycaprolactone in the polymer matrix. The optimal sample with 1% zinc oxide and 1% graphene had antibacterial properties more than other samples. Also, the survival rate of fibroblasts cell in the vicinity of the optimal matrix was significantly different from other samples.*

Conclusion*: The obtained results revealed that the incorporation of the nanoparticles improved physico-chemical features and mechanical strength with enhanced biological properties and its anti-bacterial performance makes this material a promising candidate for further bone regeneration studies.*

Keywords: *Polycaprolactone, polylactic acid, hydroxyapatite, graphene, zinc oxide.*

1. INTRODUCTION

Up to now, bone damages and failures as well as related defects have been recognized as a serious health problem by world health organization (WHO) as a result of dramatical rise in the bone diseases such as bone tumor, ageing trauma population, damages from sport activities and traffic accident (1). From realistic point of view, new advancements in fully engineered tissues have offered an alternative method to deal with bone related disease through altering damaged sites with multifunctional substitution in comparison with traditional approaches including allografts and autografts, introducing highly potential solutions to overcome the shortages of donated tissues (2-4). In addition, traditional therapies suffer from some disadvantages including disease transmission, need for further surgery, graft rejection, and pain (5). tissue engineering (TE) nanocomposite coatings support attachment, migration, and proliferation

[DOI: 10.22068/ijmse.2788]

of host cells (6). Current studies shown that many approaches and biomaterials have been tested such as natural or synthetic biomaterials, stem cells from different sources, and grafts in order to restore/ regenerate massive defects, designing a suitable three-dimensional (3D) substrate to eliminate disadvantages of the grafts (7-9). The TE nanocomposite coating is a supporting place for attachment, migration, proliferation, and differentiation of cells, and its main function is reproducing the ECM. Thus, its role to control cell behaviors and fates can result in naturally tissue regeneration (10).

Recently, various types of bio-materials have been employed in fabrication of tissue-engineered composite coating to enhance bone regeneration. For instance, He et al. fabricated collagen/ poly lactide (PLA)/ nano-hydroxyapatite composite coating to induce mesenchymal stem cells (MSCs) differentiation (11). Moreover, Oryan et al. produced β-tricalcium phosphate/ chitosan membrane to enhance bone reconstruction (12). The mentioned nanocomposite coating are designed with different types of biomaterials such as synthetic, natural, or a combination of both. It is noted that the nanocomposite coating should be designed with suitable degradation rate, mechanical stiffness, biocompatibility, and the nanocomposite coating used for TE should degrade at a rate that tuned with the rate of tissue growth (13). Polycaprolactone (PCL) and PLA as synthetic polymers have been applied to regenerate bone structure due to their mechanical properties, biodegradation rate, and biocompatibility. PLA is fragile with low elongation at break, thus, its combination with polymers such as PCL which is a stiffness polymer with higher elongation at break properties can enhance its mechanical features. On the other hand, cell/scaffold interaction of PCL is improved with the addition of PLA due to better surface energy (14-16). Therefore, fabricated composite coating can show better properties in comparison with the single polymer, however, there is still room for improvement because of its lack of functional groups and hydrophobicity in the PCL/PLA composite which need to be modified for biomedical applications. Additionally, the nanocomposite coating for bone regeneration needs having proper osseointegration and osteoinductivity potential (17). In addition, other features such as mechanical properties, hydrophilicity and biocompatibility would be improved with the combination of bioactive agents such as hydroxyapatite (HA). The addition of HA also enhances bone cells attachment, proliferation, and differentiation. Furthermore, mineralization and bone formation is increased due to its calcium components (18). Currently, various types of nanoparticle have been used to fabricate nanocomposite (19, 20). According to diverse types of nanofillers, using inorganic nanoparticles can be a wise selection because of their anti-microbial and mechanical strength properties (21, 22). Furthermore, one of the most crucial factor in the fabrication of nanocomposite with using nanoparticles is dispersion of inorganic types in the polymer matrices because it can improve composite properties drastically, which is possible with using ZnO due to its particle-particle interactions and surface energy (23). Zinc oxide (ZnO) which is approved by the Food and Drug Administration (FDA) in addition to its functional properties is semiconductor nanoparticle which can be used because of its low toxicity, chemical stability, anti-bacterial capacity and influential oxidation strength, and it is low-cost and it is known as a multifunctional inorganic nanoparticle (24-27). Moreover, graphene (Gr), a single atomic membrane, is recognized as the most versatile biomaterial due to its electrical, mechanical, optical, and thermal properties and high surface area which make this a promising material is biomedical applications (28).

Regarding the previous studies, bone tissue-like structure was fabricated by different techniques, such as electrodeposition, die cast, dip coating, spin coating, electrospinning, layer by layer assembly, freeze drying, solvent casting, covalent linkage, co-precipitation, and ionic interaction techniques (29-31). Among the above approaches, solvent casting and die casting methods, the simplest, are two specific approaches which are solution-based techniques to fabricate membrane or film for simulation of the tissue microenvironment structure (32).

In the present study, casting after solution mixing and injection molding were used in order to producing composite with different concentrations of Gr and ZnO nanoparticles as filler materials incorporating in PLA/ PCL/HA composite. The physical, chemical, and mechanical properties of the fabricated

[DOI: 10.22068/ijmse.2788]

nanocomposites were evaluated via FESEM, EDS, FTIR, XRD, contact angle, mechanical evaluation, electrical conductivity, and In vitro degradation. Then, biological properties of fabricated nanocomposite coating were analyzed, and antibacterial assessment was carried out.

2. MATERIALS AND METHODS

2.1. nanocomposite coating fabrication

The PLA/PCL, PLA/PCL/HA, PLA/PCL/HA/ZnO, and PLA/PCL/HA/ZnO/Gr membranes were fabricated via solvent casting method combined with a die cast technique (Table 1). In brief, fabrication of PPH0Z0G0 which was chosen as a control group was carried out as follows: the combination of 5 g PLA and 1.2 g PCL (80/20 w/v, 80000 g/mol, both purchased from Sigma-Aldrich) was dissolved in Chloroform (Cl, 90 mL/g, Sigma-Aldrich). After 24h under magnetic stirrer condition, the obtained solution was sonicated for 30 min at room temperature. As it is shown in table 1, fully dissolved PLA/PCL solution was further mixed and sonicated with HA/Cl (3 wt.%, Parsian Merck, Iran) solution to obtain a clear and homogenous solution. Addition of ZnO and Gr (both purchased from Parsian Merck, Iran) nanoparticles were carried out similarly. In brief, PLA/PCL, and HA were combined with Cl (3 wt.%) separately. ZnO and Gr nanoparticles also mixed with Cl (3 wt.%) separately. Finally, all thoroughly mixed solutions were combined followed by using sonication for 30 min.

The membrane was fabricated through using solvent casting technique, then die casting membranes was produced, the prepared mixtures were purred onto glass petri-dishes after evaporation of solvent at room temperature (37°C), and vacuum oven was used for completely removed excess solvent for 48 h, further stored for further studies.

2.2. Morphological studies

To detect and evaluate the incorporation of nanoparticles into the films plus the nanoparticles surface area, pore size, pore volume, and cross section micrographs were visualized with field emission scanning electron microscope (FESEM, TESCAN-Vega 3, Czech Republic) equipped with energy dispersive spectroscopy (EDS) at 20 kV. Before morphological assessment, the prepared films mounted on the brass stub and sputtered coated under a flow of argon to enhance the conductivity of the samples.

2.3. Mechanical strength

Regarding the standard ASTM-D638, mechanical properties of fabricated films were determined via a Texture Analyzer TA. XT plus (TM–SM, Instron, UK) by a 50 N load cell under a crosshead speed of 50 mm/min. the tensile strength and elongation at break were evaluated in 5 specimens from each of the produced films. Fabricated nanocomposite coatings also were evaluated in the wet state to observe the mechanical response into *in vivo* condition. To reach this purpose; the mechanical test was carried out after soaking the films in PBS for 48h. each sample were assessed after five times repetition.

2.4. Chemical structure investigation

The functional groups of the prepared membranes were investigated via Fourier transform infrared spectrometer (FTIR, Nicolet, NEXUS 670, USA) In the range of 400-4000 cm^{-1}.

2.5. Hydrophilicity Studies

To observe the hydrophilicity of different samples, contact angle meter (XCA-50) was used. In brief, samples were analyzed and reported after 15s of water dropping through using a water droplet with a volume of 4 µL. The reported results were based on the average of five times repetition.

2.6. Electrical conductivity

To evaluate the electrical conductivity of the nanocomposite coatings, four steel blades were placed on the membranes. The associated conductivity (δ) was accomplished based on Pouillet's law (28) as follows (Eq. 1): resistance (R) and Electrical conductivity (EC) were assessed five times for different samples individually.

$$\delta = L/(R \times A) \quad (1)$$

where A, and L were considered as the surface area, and length of the fabricated samples, respectively.

2.7. Characterization of the nanoparticles and films

To assess nanoparticles incorporated PPH0Z0G0, PPH1Z0G0, and PPH1Z0.5G0.5 membranes, structural analysis was accomplished via X-ray diffraction (XRD, STOE, IP-PSD).

[DOI: 10.22068/ijmse.2788]

2.8. In vitro degradation

To measure the biodegradation behavior of the membranes, the fabricated nanocomposite coatings (n=5) were similarly cut ($5 \times 5 \times 3$ mm^3), weighed (W_0), and soaked in PBS (Ph = 7.4), and after that the incubation process was carried out at 37 °C with continuous shaking at 50 rpm for 14 days. This should be mentioned that the PBS was changed at each interval time point. To assess the weight loss, at different time point (3, 7, and 14 days), the samples were transferred for elimination of excess water, next rinsed with distil water (DW), then dried at vacuum oven at 37°C and weighed (W_d). The calculation of weight loss was carried out regarding the following equation (Eq. 2) (33):

$$\Delta W\ (\%) = \frac{W_0 - W_d}{W_0} \times 100\% \qquad (2)$$

2.9. Calcium and zinc release

Ca and Zn ions release from the nanocomposites was evaluated by using coupled plasma-optical emission spectrum (ICP-OES, Pekin Elmer-Optima 7300 DV). The nanocomposites were cut into similar dimensions, then soaked into SBF (10 mm, n=5). After that, the ion release profile was observed in 3, 7, and 14 days.

2.10. Bioactivity evaluation

To observe the bioactivity of the nanocomposite coatings, fabricated membrane with equal dimension (5× 5 mm^2) was placed into completely sterilized petri dishes, and then soaked in SBF (Ph = 7.4) at room temperature for four weeks. After that, at each preselected time, they were dried at 37 °C, and then analyzed with SEM and XRD to observe the formation of HA crystal, and its depositions. In addition, the amount of Ca, Zn, and P ions was calculated via ICP-OES in the SBF.

2.11. Biological performance

Mouse fibroblast (L929, Pasteur, Iran) was used as a cell line. In order to cell culture, briefly, the collected cells were seeded in Dulbecco's Modified Eagle Medium/Nutrient Mixture F-12 (DMEM-F12, Gibco, USA) medium, 1% antimycotic and antibiotic formulation, 1% L-glutamine (all from Gibco, USA), with 10% fetal bovine serum (FBS; BIOCHROM AG, Germany), containing amphotericin B, streptomycin sulfate, and penicillin G sodium (all from Invitrogen). After covering plates with cells, the cultured cells were rinsed two times with 4 mL PBS. After that, detachment of cells was carried out by EDTA/trypsin, then the cells were centrifuged (1200 rpm, 4 min). The obtained cells were cultured and incubated again. The culture medium (37 °C in a humidified condition with 5% CO_2) was changed every two days.

The cytotoxicity assessment (MTT assay, Sigma-Aldrich) was carried out to observe lived-dead cells. First, the membranes were cut into disk shapes equally, then placed into 24-well plate. Then, the samples were placed into incubator (37°C for 24 h). After that, they (L929 with a density of 10×10^3) were cultured, and incubated onto each sample. It should be noted that the medium was changed at each 3-4 days. To evaluate MTT assessment, the culture medium was removed, and the samples were washed by PBS three times. Next, 50 µL MTT and 500 µL medium was added to each plate. after incubation (37°C for 3-4 h), the medium was extracted, and 400 µL DMSO (Sigma-Aldrich) was replaced to the wells. Then, the obtained solution was pipetted and placed in the dark condition (depended on the detachment rate of cells). as the final step, Elisa reader (570 nm wavelength, Bio-Rad, C55, Germany) was employed to assess with transferring 100 µL of each sample to 96-well plate (n=5) based on revived formazan in 24 and 72 h. The cell viability (%) was evaluated by Eq. (3):

$$\text{Cell viability}\ (\%) = \frac{OD_{Sample}}{OD_{Control}} \times 100\% \qquad (3)$$

2.12. In vitro anti-microbial assessment

The antimicrobial efficiency of the nanocomposite membranes was assessed against *E. coli* and *S. aureus* as Gram-negative and Gram-positive, respectively, with association of the zone of inhibition technique (34). Briefly, in vitro anti-microbial evaluation, a multi-step protocol was carried out one after another as follows: (1) dipping the membranes; (2) incubation of the inoculums; (3) shaking the tubes at room temperature; (4) extracting the aliquots; (5) diluting the samples serially by PBS and then spreading onto the plates; (6) incubation of the plates at room temperature for 24h. Finally, the colony-forming units were calculated. PLA/PCL was used as a control sample.

2.13. Statistical analysis

All reported experimental data were arranged on mean and standard deviation (±SD). In addition, SPSS software and a one-way ANOVA test were

[DOI: 10.22068/ijmse.2788]

used to assess cellular data. It should be mentioned that, $p \leq 0.05$ was recognized statistically substantial.

3. RESULTS AND DISCUSSIONS

3.1. PLA / PCL / HA / ZnO / Gr nanocomposite coating fabrication

Over this section, different steps of nanocomposite fabrication are described. Producing PLA/PCL/HA/ZnO/Gr with optimized properties was the main purpose, however this needs step by step evaluation. Thus, our first goal was to explore a proper weight ratio between PLA/PCL/HA and ZnO, and Gr to produce a nanocomposite coating with sufficient mechanical, chemical, morphological, physical, and biological properties because the mentioned nanoparticles and polymers are introduced biocompatible for tissue engineering applications. First step was optimization of ZnO with PLA/PCL/HA through three weight ratiosas described in Table 1 in addition HA was evaluated for the combination of PLA/PCL to find which one would generate the nanocomposite with promising properties. The FESEM micrographs and cross-sections of fabricated nanocomposite coatings are shown in Fig. 1 and Fig. 2, where the effect of HA, ZnO, and Gr addition to the PLA/PCL membrane is obvious. Furthermore, the textural properties pore size (µm) and mechanical properties elongation (%), ultimate tensile strength (UTS, MPa), young's modulus (MPa), and wettability of fabricated membranes are shown through Table 2 and 3, respectively. According to the Fig. 1 and Table2, the PLA/PCL nanocomposite revealed homogenous and similar interconnected pore size ~ 1.52 µm. With combination of HA, the pore size was increased up to ~ 1.82 µm, increasing surface flexibility without risk of early degradation, which promote membranes adoptability features for further studies (35). As it is visible, the addition of ZnO affects the morphological properties, raising in the nanoparticles content up for PPH1Z0.1G0, PPH1Z0.5G0, and PPH1Z1G0 promoted pore size to ~ 2.51, 2.84, and 3.66 µm, which may be the consequences of reducing interaction between polymers and ZnO, which is normal in the combination of nanoparticles into membranes (36). Then, Gr incorporation further showed better distribution and encouraging up for PPH1Z0.1G0.1, PPH1Z0.5G0.5, and PPH1Z1G1 to ~ 3.01, 3.27, and 4.01 µm, and its morphological properties were proper in shape. Our major focus was based on using the maximum percentages of nanoparticles because of positive effect on mechanical, chemical, and biological properties without any cytotoxicity. Therefore, our further investigations were based on blending 1 wt.% ZnO and 1 wt.% Gr with the prepared membrane. Fig. 2 illustrated the pores of prepared nanocomposite coatings were interconnected, and their shapes were irregular in structure with different properties. However, the addition of ZnO and Gr affects positively in the structure with good textural properties which could revealed proper mechanical, chemical and biological features.

Appropriate mechanical performance such as compressive strength, fatigue strength, tensile strength, shear modulus, toughness and young's modulus are the most noticeable features in bone tissue regeneration (37).

Table 1. Composition of prepared membranes.

Sample	Composition	PLA/PCL (w/v)	Hydroxyapatite (w/v)	Zinc oxide (w/v)	Graphene (w/v)
PPH0Z0G0	PLA/PCL	80/20	–	–	–
PPH1Z0G0	PLA/PCL/HA	80/20	1 %	–	–
PPH1Z0.1G0	PLA/PCL/HA/ZnO	80/20	1 %	0.1 %	–
PPH1Z0.5G0	PLA/PCL/HA/ZnO	80/20	1 %	0.5 %	–
PPH1Z1G0	PLA/PCL/HA/ZnO	80/20	1 %	1 %	–
PPH1Z0.1G0.1	PLA/PCL/HA/ZnO/Gr	80/20	1 %	0.1 %	0.1 %
PPH1Z0.5G0.5	PLA/PCL/HA/ZnO/Gr	80/20	1 %	0.5 %	0.5%
PPH1Z1G1	PLA/PCL/HA/ZnO/Gr	80/20	1 %	1 %	1 %
PPH1Z1G2	PLA/PCL/HA/ZnO/Gr	80/20	1 %	1 %	2 %

[DOI: 10.22068/ijmse.2788]

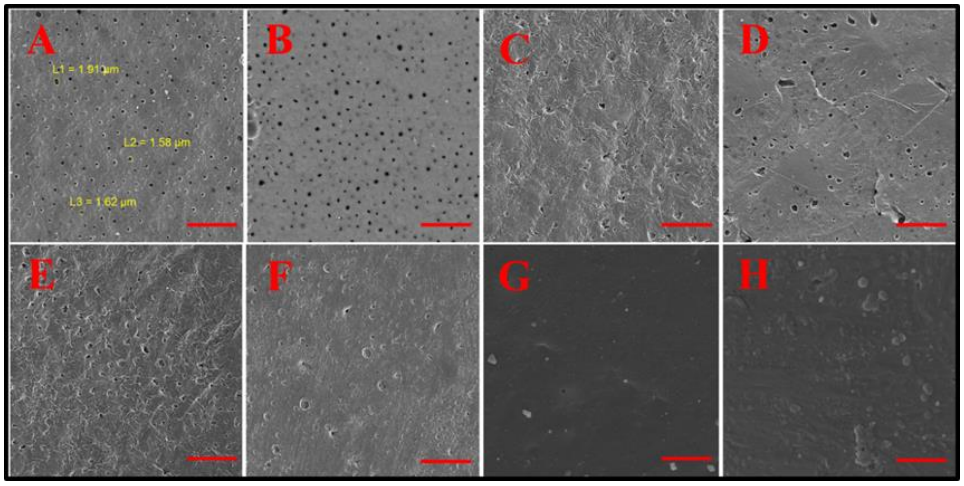

Fig. 1. FESEM micrographs of PPH0Z0G0 (A), PPH1Z0G0 (B), PPH1Z0.1G0 (C), PPH1Z0.5G0 (D), PPH1Z1G0 (E), PPH1Z0.1G0.1 (F), PPH1Z0.5G0.5 (G), and PPH1Z1G1 (H) prepared membranes. Scale bar was 20 µm.

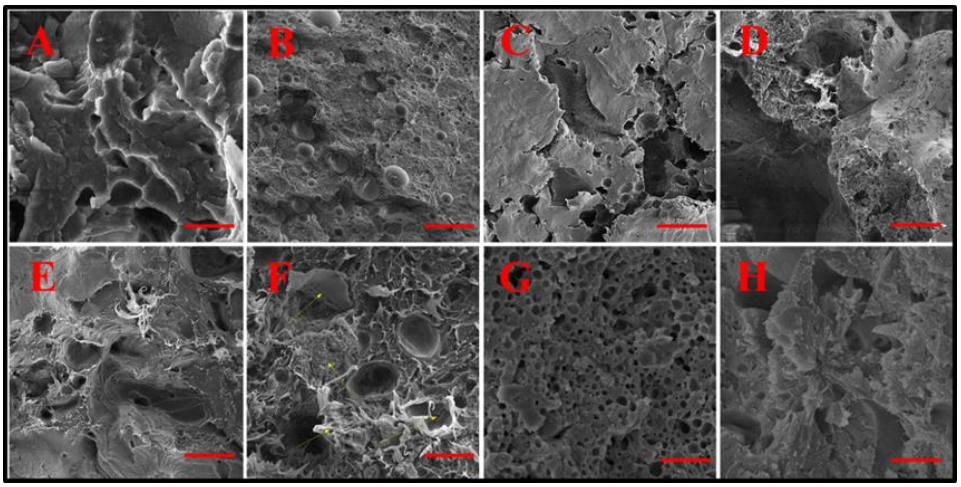

Fig. 2. Cross section of PPH0Z0G0 (A), PPH1Z0G0 (B), PPH1Z0.1G0 (C), PPH1Z0.5G0 (D), PPH1Z1G0 (E), PPH1Z0.1G0.1 (F), PPH1Z0.5G0.5 (G), and PPH1Z1G1 (H) prepared membranes. Scale bar was 20 µm.

Table 2. The textural properties of PLA-PCL, PLA-PCL-HA, PLA-PCL-HA-ZnO, and PLA-PCL-HA-ZnO-Gr membranes

Sample	Pore size (µm)
PPH0Z0G0	1.52 ± 0.241
PPH1Z0G0	1.82 ± 0.146
PPH1Z0.1G0	2.51 ± 0.501
PPH1Z0.5G0	2.84 ± 0.257
PPH1Z1G0	3.66 ± 0.71
PPH1Z0.1G0.1	3.01 ± 0.917
PPH1Z0.5G0.5	3.27 ± 1.122
PPH1Z1G1	4.01 ± 0.564

Sufficient mechanical behavior to withstand stress after implantation (maintaining its features during the surgical process), and keeping its microstructure during of new bone formation. Therefore, having enough mechanical properties in wet state plus dry state are of great importance (36). The mechanical properties of PLA/PCL incorporated nanoparticles are summarized in

[DOI: 10.22068/ijmse.2788]

Fig. 2 and Table 3 in both dry condition and after soaking membranes into SBF, representing that incorporation of nanoparticles enhanced tensile strength significantly.

The enhancement of young's modulus is generally associated with lower interfacial energy between the nanoparticles and polymer matrix (38, 39). Although nanoparticles incorporation resulted in improving mechanical properties in dry and wet state, as it was revealed its Young's modulus was decreased with addition of 2% Gr, which could be because of agglomeration effect (40).

Thus, PPH1Z1G1 nanocomposite presented the best mechanical performance among different percentages of nanoparticles in terms of UTS= 20.91 ± 1.001 MPa and young's modulus= 1742.5 ± 316.541 MPa in dry state, and UTS= 13.17 ± 0.458 and young's modulus= 1097.5 ± 71.412 in wet state.

As synthetic materials are known as a material with hydrophobic components, this feature is valued disadvantage as far as natural bone tissue reconstruction is needed (17). To solve this, there have been some approaches such as surface treatment, adding bioceramics, and combination with natural polymers can be used.

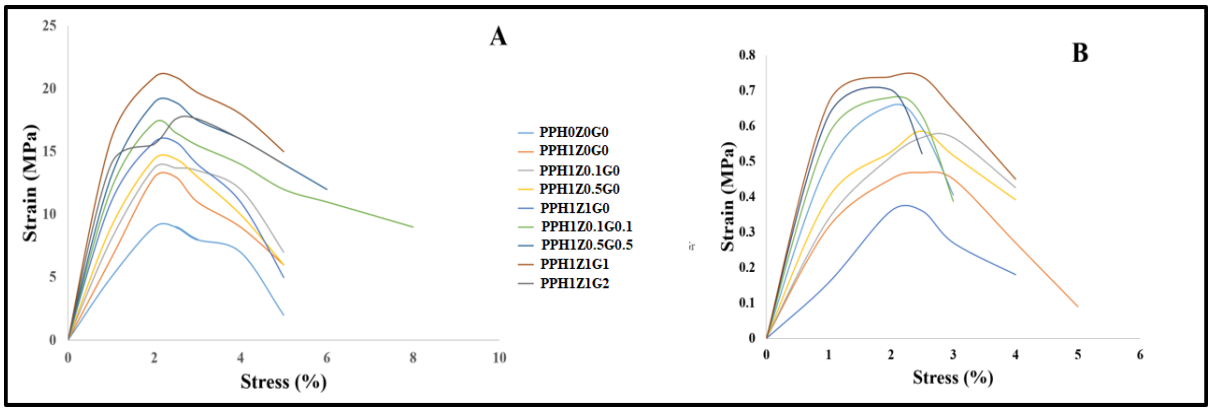

Fig. 3. The stress-strain curves of prepared membranes in dry (A) and wet (B) conditions.

Table 3. Mechanical properties and wettability of PLA-PCL, PLA-PCL-HA, PLA-PCL-HA-ZnO, and PLA-PCL-HA-ZnO-Gr membranes.

Sample	Young's Moudulus (%)		UTS(Mpa)		Elongation (%)		Water contact angle (°)
	Dry	Wet	Dry	Wet	Dry	Wet	
PPH0Z0G0	450 ± 87.176	350.24 ± 52.102	9 ± 0.538	8.12 ± 0.301	5.1 ± 0.417	4.9 ± 0.311	89 ± 0.103
PPH1Z0G0	648.5 ± 92.613	542.83 ± 23.412	12.97 ± 0.451	10.58 ± 0.249	4.7 ± 0.339	4.5 ± 0.389	86 ± 0.271
PPH1Z0.1G0	720.5 ± 91.312	590.12 ± 31.175	13.7 ± 0.508	11.23 ± 0.327	5.2 ± 0.408	5 ± 0.409	86 ± 0.569
PPH1Z0.5G0	953.33 ± 93.981	680.75 ± 36.567	14.41 ± 0.672	10.28 ± 0.238	5 ± 0.412	4.9 ± 0.389	83 ± 1.329
PPH1Z1G0	1050.66 ± 104.052	782.661 ± 43.734	15.76 ± 0.717	11.74 ± 0.389	5.3 ± 0.441	5.2 ± 0.341	75 ± 0.153
PPH1Z0.1G0.1	1017.64 ± 112.719	678.45 ± 38.378	17.3 ± 0.919	11.533 ± 0.372	6.2 ± 0.628	6.1 ± 0.506	84 ± 2.181
PPH1Z0.5G0.5	1260.66 ± 213.306	854.54 ± 62.701	18.91 ± 0.837	12.81 ± 0.439	6.5 ± 0.672	6.3 ± 0.595	90 ± 2.454
PPH1Z1G1	1742.5 ± 316.541	1097.5 ± 71.412	20.91 ± 1.001	13.17 ± 0.458	5.3 ± 0.462	5.3 ± 0.468	78 ± 1.232
PPH1Z1G2	1350 ± 240.112	981.21 ± 69.543	19.5 ± 0.994	12.1 ± 0.389	5.2 ± 0.451	5 ± 0.371	114 ± 3.651

[DOI: 10.22068/ijmse.2788]

To measure the effect of nanoparticles addition on the hydrophilicity of PLA/PCL nanocomposites, the wettability test was considered. The water contact angle (WCA) data is shown in Table. 3. The WCA of PLA/PCL was about 89°. The combination of HA with polymeric matrix enhanced hydrophilicity to about 86°. The further measurement showed that the WCA of PPH1Z0G0, PPH1Z0.1G0 and PPH1Z0.5G0 were about 86, 83 and 75°, respectively. Although addition of ZnO improved wettability of nanocomposites because it resulted in the larger micro-pores, its hydrophilicity improvement was not significant (41). After that, the hydrophilic properties of nanocomposite coatings also improved with addition of Gr, proving sufficient performance with increasing amount of Gr (42). Results demonstrated that well-dispersed ceramic nanoparticles in scaffold improved hydrophilicity and mechanical properties compared with agglomerated ceramic nanoparticles. In this research agglomeration has happen in the structure of PPH1Z1G2 scaffold (2% Gr), that caused to decrease mechanical properties and increase hydrophobicity (6, 43).

Regarding the mentioned properties of ZnO/Gr-incorporated PLA/PCL/HA nanocomposite coating, it was exposed that PPH1Z1G1 showed outperforming properties than the others in morphological, chemical, and mechanical stability. Therefore, PLA/PCL/HA with incorporation of 1 wt.% ZnO and 1 wt.% Gr was considered as an optimized sample and the cell compatibility performance—bioactivity, biodegradation, and cell viability—were evaluated experimentally and compared with those of PLA/PCL and PLA/PCL/HA nanocomposite samples.

3.2. The PLA / PCL / HA (1 wt.%) /ZnO (1 wt.%) / Gr (1 wt.%) nanocomposite coating

The chemical groups of different membranes - PLA/PCL, PLA/PCL/HA, PLA/PCL/HA/ ZnO, PLA/PCL/HA/ ZnO/Gr - were evaluated through FTIR and the collected results are shown in Fig. 4, where the FTIR spectrum of PCL correspond to the CH_2 asymmetric and symmetric, and carbonyl stretch, C-O stretch were at 2860, 2940, 1720, and 1271 cm^{-1}; while, at 1720, 2883, and 1032 cm^{-1} represent carbonyl stretch, CH3 stretch, and C-O stretch of PLA, respectively. Moreover, Fig. 4(b) represented the spectrum of HA where $PO4^{-3}$ stretch band, and OH stretch was around 974 and 3500 cm^{-1}, respectively (10, 44). Fig. 4(c) bands at 1370 cm^{-1} showed symmetric and 1600 cm^{-1} illustrated asymmetric stretches. However, additional peak was not revealed after mixing ZnO into membrane as it was reported earlier by Shankar et al. and Huang et al. for PLA/ZnO film (41, 45, 46). Functional groups of Gr also appeared at 1530 and 1550 cm^{-1} proves represented the vibrational band G and asymmetric tensile vibration of the C-C bond, respectively (47-49).

The XRD evaluations of PLA / PCL / HA, PLA / PCL, and PLA / PCL / HA / ZnO / Gr membranes are revealed in Fig. 5. Illustrating the XRD peaks of ZnO and Gr nanoparticles hither was due to proving completely distinguishing the nanoparticles in the nanocomposite's pattern. Two distinguishable peaks of PLA and PCL were observed in the range at 16.5° and 18.8° (50). The mentioned peaks also can be seen in XRD observation of ternary PLA/PCL/HA nanocomposite with some changes. However, the distinguishable peaks at 26°, 31.63°, 32.42°, and 33.25° through hexagonal shapes can prove HA composition (51). The crystalline phase of PLA/PCL/HA/ZnO/Gr nanocomposite was assessed via X-ray diffraction test. The PLA/PCL/HA are shown with some changes. The distinguishable peaks of ZnO were observed at 31.9°, 33.4°, 47.1°, 56.1°, 63.1° (52), In addition, peaks at 25.8° (002) and at 42.7° (101) in Fig. 5, were assigned to f hexagonal wurtzite geometry in ZnO (JCPDS 36-1451) (53) . and the diffraction peaks of Gr at 10.69°, while no other crystalline peaks were observed related to Gr (54).

Fabricating nanocomposite with the best chemical, mechanical, physical, and biological properties is the foremost reason of incorporation of nanoparticles into polymeric components (55). From materialistic point of view, nanoparticles such as ZnO and Gr are well-known to enhance the cell/scaffold interaction like cell adhesion, proliferation, and growth because of offering some functional ions in order to simulating native ECM.

[DOI: 10.22068/ijmse.2788]

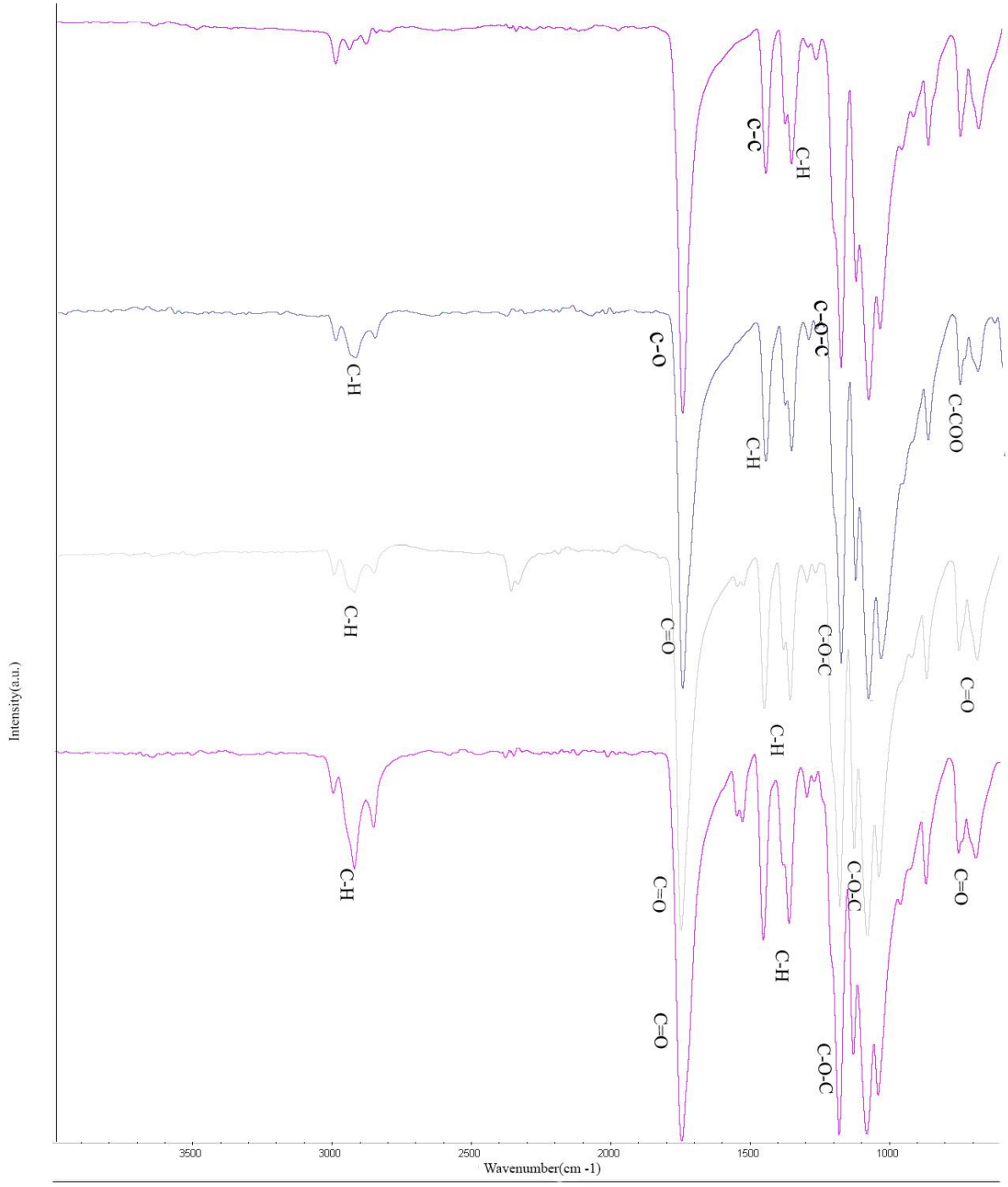

Fig. 4. The FTIR spectra of PLA-PCL (A), PLA-PCL-HA (B), PLA-PCL-HA-ZnO (C), and PLA-PCL-HA-ZnO-Gr (D).

[DOI: 10.22068/ijmse.2788]

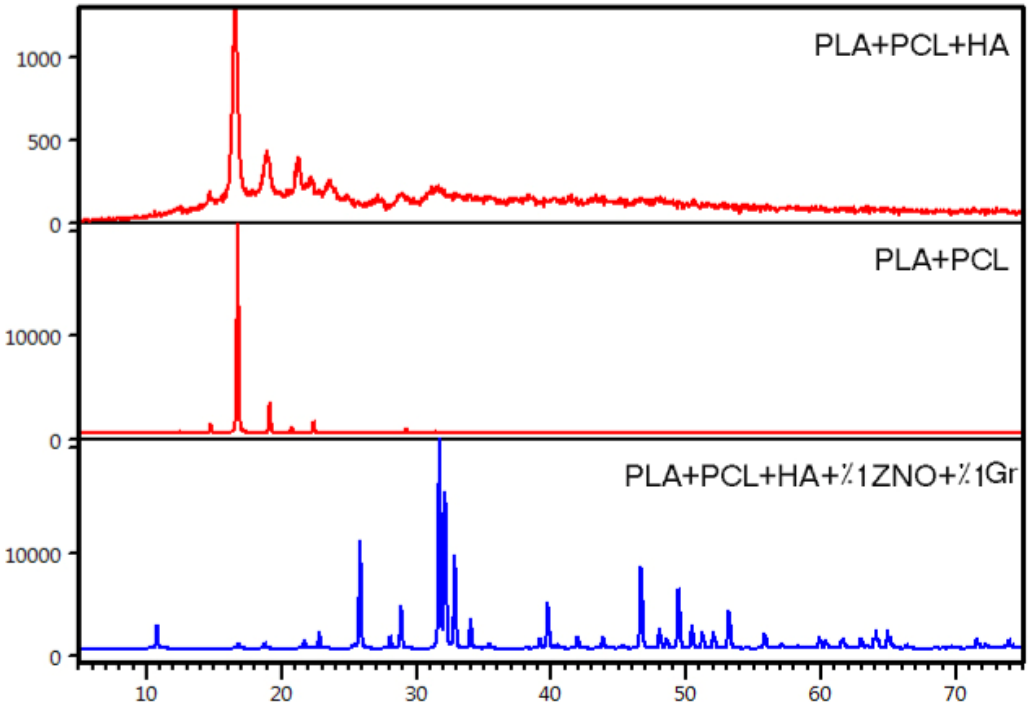

Fig. 5. The XRD patterns of PLA-PCL, PLA-PCL-HA, and PLA-PCL-HA-ZnO-Gr nanoparticles.

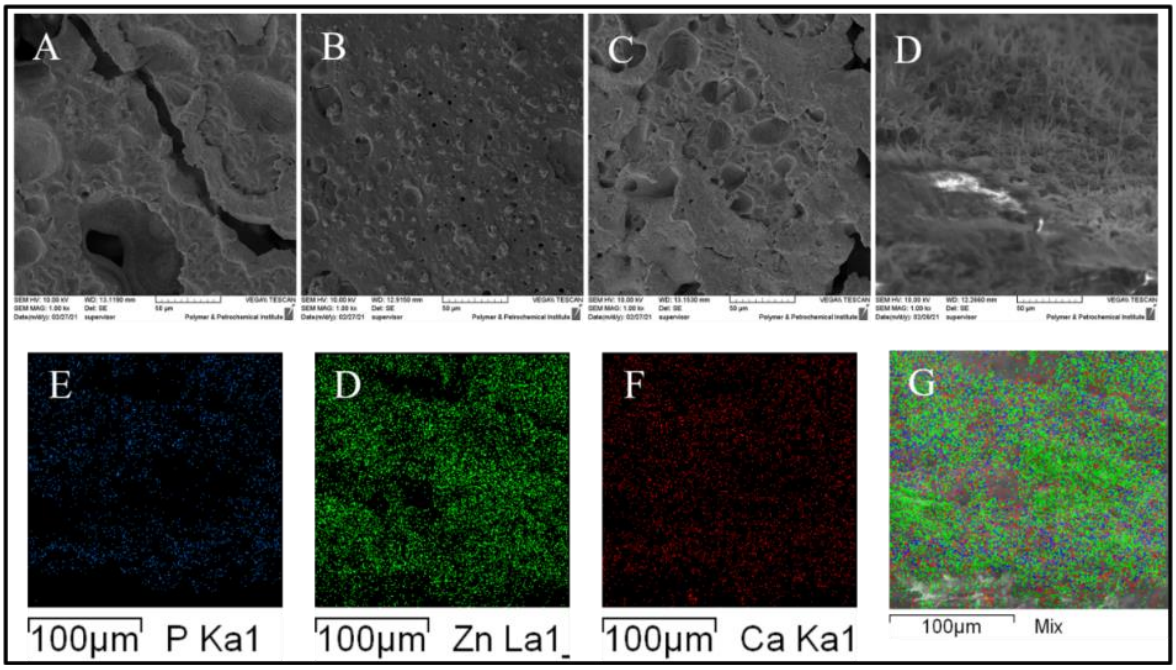

Fig. 6. the FESEM micrographs relating to bioactivity potential of PLA-PCL (A), PLA-PCL-HA (B), PLA-PCL-HA-ZnO (C), and PLA-PCL-HA-ZnO-Gr (D), and EDS analyses of PLA-PCL-HA-ZnO-Gr (E, F, G, and H).

Furthermore, guaranteeing osteointegration with the host targeted sites is considered as an ideal bone membrane because this tissue-engineered nanocomposite coating can bring active environment to form calcium phosphate layer on the surface. The generated layer will impact positively to make a functional bond between the nanocomposite coating and host bone. Thus, bone tissue regeneration will be happening (56). One of the most reliable ways to simulate the formation

[DOI: 10.22068/ijmse.2788]

of calcium phosphate layer of fabricated nanocomposite coatings is to soak them into the SBF over some preselected times (57). In the present study, this method was carried out to evaluate the apatite nucleation and growth potential of PLA/PCL, PLA/PCL/HA, PLA/PCL/ZnO, and PLA/PCL/ZnO/Gr membranes up to 60 days experimentally. After 60-days submerging, nanocomposite coatings were evaluated through SEM micrographs. Furthermore, the elemental assessment was considered to prove calcium phosphate newly formation. The obtained results are involved the SEM micrographs of PLA/PCL, PLA/PCL/HA, PLA/PCL/HA/ZnO, and PLA/PCL/HA/ZnO/Gr, and EDS analyses of PLA/PCL/HA/ZnO/Gr nanocomposite are illustrated in Fig. 6. As it is obvious, with increasing time up to 60 days, calcium phosphate was formed on different nanocomposite coatings, especially on the PPH1Z1G1 surface. Interestingly, the calcium phosphate layer of PLA/PCL/HA/ZnO/Gr was totally formed on the surface. In addition, the EDS test proved that nanocomposite coatings were covered mostly with phosphorus and calcium, which showed calcium phosphate formation on the PLA/PCL/HA/ZnO/Gr nanocomposite coating. The collected results of bioactivity assessment revealed that the nanoparticles loaded in PLA/PCL membrane resulted in inducing the bioactivity kinetic substantially.

According to current studies, the cell/scaffold interaction can be improved with increasing the electrical conductivity of fabricated nanocomposite coatings (58). Moreover, addition of electro-conductive nanoparticles prevents the agglomeration of nanoparticles, improving chemical and physical properties of membrane. Thus, electrical conductivity of fabricated membranes was investigated as described above, and Table 4 presented addition and higher amount of Gr is a main reason to enhance the electrical properties. The release profile showed that, after the nanocomposite coating was placed into SBF solution, Ca ions were released. The results at each interval times are shown in Fig. 7. First and foremost, the nanoparticles loaded weight ratio into PLA/PCL/HA nanocomposite coatings were estimated. To calculate this, the weight of fabricated membranes was fixed about 2 mg. Thus, the weight of Ca and Zn were approximately 450, and 550 µg for PPH1Z1G0 and PPH1Z1G1, respectively. After that, the membranes were weighed after removing from the solution through ICP. The release profile was assessed for both Ca and Zn ions separately. For Ca ion, after one week the rate of release was about 91, 93.5, and 74 mg/l, and for Zn ion was about 0.01, 8.5, and 8.6 mg/l for PPH1Z0G0, PPH1Z1G0 and PPH1Z1G1, respectively. Moreover, the Ca ion release was raised in duration of 14 days for both PPH1Z1G0 and PPH1Z1G1, however, it was more noticeable for PPH1Z1G1 (about 176 mg/l). Furthermore, Zn release for PPH1Z1G0 was more substantial (about 147 mg/l) in comparison with PPH1Z1G1, which was increased steady.

One of the most noticeable properties of tissue engineered nanocomposite coating for bone tissue regeneration is having adjustable in vitro degradation, and this must to be tuned with bone newly formation, which has a noticeable impact on nanocomposite coating applicability (59). The *in vitro* degradation of fabricated nanocomposites including PLA / PCL, PLA / PCL / HA, PLA/PCL/HA/ZnO, PLA/PCL/HA/ZnO/Gr was evaluated into PBS aqueous solution up to 20 weeks. It is proved that PLA/PCL showed biodegradation rate slowly which can be found in Fig. 8. After HA blending into PLA/PCL nanocomposite coating, the rate of degradation was increased due to improving hydrophilicy of membrane. It should be mentioned that degradation rate of the nanocomposite coating like pure PLA/PCL as a control sample can be used to observe the positive effect of combination of HA into nanocomposite coating because the nanocomposite coating had degraded approximately 6.48 % of its weight up to 20 weeks.

Table 4. Electrical conductivity of PLA-PCL, PLA-PCL-HA, PLA-PCL-HA-ZnO, and PLA-PCL-HA-ZnO-Gr membranes

Sample	Electrical conductivity (S/M)	probability
PPH0Z0G0	0.00046 ± 0.00097	0.016
PPH1Z0G0	0.00055 ± 0.0007	0.017
PPH1Z1G0	0.007122 ±0.0013	0.007
PPH1Z1G1	0.010416 ± 0.012	<0.005

[DOI: 10.22068/ijmse.2788]

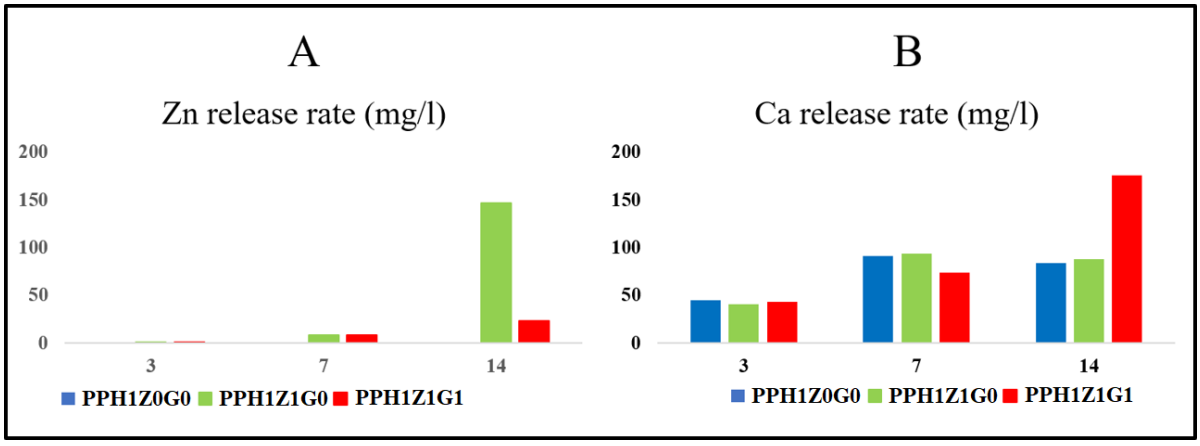

Fig. 7. The Zn (A) and Ca (B) release profile of PLA-PCL-HA, PLA-PCL-HA-ZnO, and PLA-PCL-HA-ZnO-Gr.

After careful evaluation of PPH1Z1G0 and PPH1Z1G1 nanocomposite coatings, the *in vitro* degradation of the nanocomposite coatings was increased to about 8.92 and 9.31 % after the end of period, respectively. It can be concluded that after soaking them into PBS, the nanoparticles were undergone this process in addition of PLA/PCL, and the nanocomposite coatings revealed a continuous and higher biodegradation rate than PLA/PCL membrane. The duration of degradation of polylactic acid in the human body is about 11 months, and this time is consistent with bone regeneration. [38].

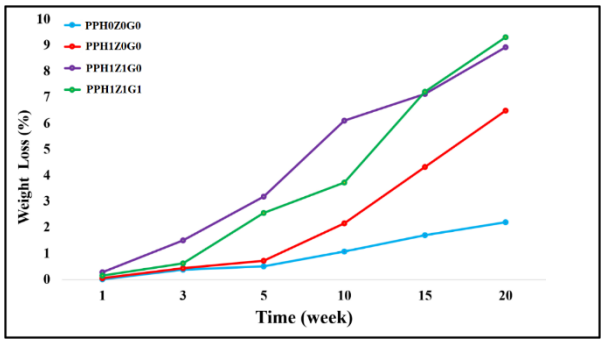

Fig. 8. The biodegradation of PLA-PCL, PLA-PCL-HA, PLA-PCL-HA-ZnO, and PLA-PCL-HA-ZnO-Gr membranes into PBS aqueous solution up to 20 weeks.

3.3. Cell compatibility

3.3.1. MTT assessment

The cell/scaffold response of PPH0Z0G0, PPH1Z0G0, PPH1Z1G0, and PPH1Z1G1 nanocomposites was evaluated *in vitro* up to three days. MTT results were shown in Fig. 9 and negative-control was chosen as the one sample which was compared with other membranes. After one day of cell culture, the samples showed better cell viability in comparison with the control sample, however there was a significant difference between the control sample and PPH1Z1G1. With increasing in the cell seeding period, the cell viability of membranes and especially those which contain ZnO (1 wt.%) and (Gr wt.%) enhanced significantly than the other samples. Pure PLA and PCL are known as biocompatible materials and it is obvious that PCL or PLA can interact with cells. However, the incorporated HA affects positively on cell/scaffold interaction. Moreover, the incorporation of ZnO and Gr nanoparticles induced cell viability, which may be because of better hydrophilicity as well as being functional co-factor for some enzymes, affecting osteogenic biomarkers by activating the bone regeneration (60, 61). Furthermore, Zn^{2+} is well-known as an important factor in order to enhancement of healthy bone regeneration (35, 62). Thus, it can be proved that cells can be affected positively by realizing these ions from the nanocomposite.

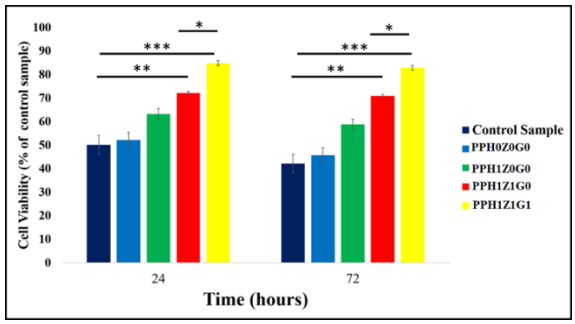

Fig. 9. The cell proliferation and viability of PLA-PCL, PLA-PCL-HA, PLA-PCL-HA-ZnO, and PLA-PCL-HA-ZnO-Gr membranes up to three days; * $P \leq 0.05$, ** $P \leq 0.01$, *** $P \leq 0.001$, **** $P \leq 0.0001$.

[DOI: 10.22068/ijmse.2788]

3.3.2. *Antibacterial assessment*

The antibacterial performance of PPH0Z0G0, PPH1Z0G0, PPH1Z1G0, and PPH1Z1G1 nanocomposites against *S. aureus* and *E. coli* were carried out with zone of inhibition technique. Its results are shown in Fig. 10 and Table 5, showing the antibacterial performances of the nanocomposite coatings. PPH0Z0G0 and PPH1Z0G0 revealed less inhibition of bacterial growth, while PPH1Z1G0 and PPH1Z1G1 showed better performance, with the rates of 37.97± 0.318 and 47.62± 0.571 mm against *S. aureus*, and 38.72± 0.341 and 49.4± 0.512 mm against *E. coli*, respectively. Regarding the current reports, the antibacterial activities of PPH1Z1G1 consists of not just the direct influence of ZnO nanoparticles but it was improved by zinc ions releasing mechanism as well as producing reactive oxygen species (ROS) (63-65). Moreover, Gr is a storage site for Zn^{2+} released from ZnO nanoparticles and enhanced the rate of permeability of the cells by having contact with negative bacteria, which finally caused cell deformation, and then leakage. Additionally, some studies have shown that ZnO can lead to lipid and protein peroxidation and further DNA damage. Gr also due to its unique structure could improve the electron transfer rate, which make this nanocomposite with higher antibacterial activities (66-69).

3.3.3. *osteoblasts attachment*

To observe the cell attachment, the produced optimal nanocomposite were sterilized as follows: the nanocomposite soaked thoroughly into PBS solution containing 20 µg/ml Erythromycin, 3 µg/ml amphotericin B, 20 µg/ml gentamicin, 50 µg/ml penicillin. Then, osteoblasts cells were cultured at 37°C for 24 h, as discussed above. To stabilize the cultured cells, glutaraldehyde (Sigma-Aldrich, USA) was added and the cells were dehydrated by methanol solution. After that, the nanocomposite was treated with tetraoxide osmium for 3 h. as the final step, and was dried before SEM assessment. The field emission scanning electron microscope image is shown in Figure 11. As you can see in Figure 11 the osteoblast cell is completely flattened on the surface. The cell has a philopedia and is completely attached to the surface. In a study by Feng et al., The addition of hydroxyapatite to a polylactic acid / polycaprolactone polymeric matrix improved osteoblast adhesion on the matrix surface (70). The results of this study are consistent with the results of research conducted by other researchers.

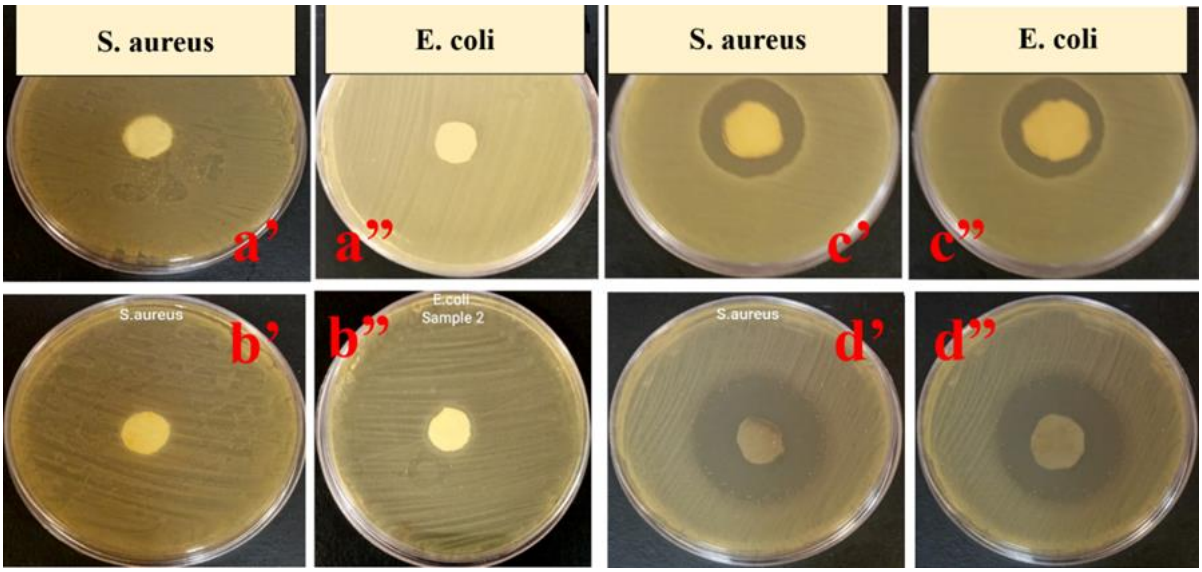

Fig. 10. The schematic anti-bacterial test of the PLA-PCL (a' and a"), PLA-PCL-HA (b' and b"), PLA-PCL-HA-ZnO (c' and c'), and PLA-PCL-HA-ZnO-Gr (d' and d") membranes against *S. aureus* and *E. coli*, respectively.

[DOI: 10.22068/ijmse.2788]

Table 5. A detailed of anti-bacterial performance of PLA-PCL, PLA-PCL-HA, PLA-PCL-HA-ZnO, and PLA-PCL-HA-ZnO-Gr membranes.

Samples	S. aureus (mm)	E. coli (mm)
PPH0Z0G0	17.42± 0.32	14.79± 0.219
PPH1Z0G0	19.35± 0.218	20.82± 0.209
PPH1Z1G0	37.97± 0.318	38.72± 0.341
PPH1Z1G1	47.62± 0.571	49.4± 0.512

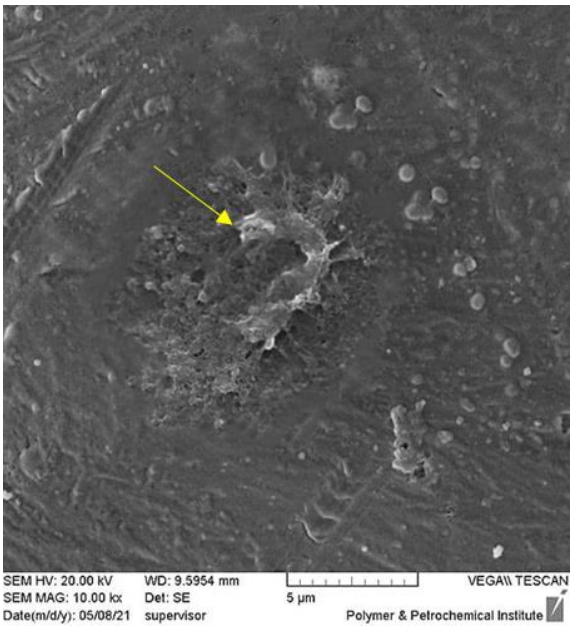

Fig. 11. The FESEM image relating to osteoblaste cell adhision on the surface of optimum sample.

4. CONCLUSION

The current experimental research was accomplished through applying two nanocomposite coating preparation techniques, but aligned in order to optimizing ZnO and Gr nanoparticles loaded into PLA/PCL/HA nanocomposite coating to fabricate a multifunctional membrane for bone defect regenerations. The weight ratio of ZnO and Gr nanoparticles were optimized; according to mechanical, morphological, and chemical characteristics. Consequently, the optimized nanocomposite coatings were considered for further studies to observe bioactivity, release profile, biodegradation, anti-bacterial performance, and cell/scaffold interaction and compared to pure PLA/PCL, and PLA/PCL/HA nanocomposite coatings. The results showed that incorporating ZnO and Gr nanoparticles improved physico-chemical properties as well as biological performance containing cell viability, proliferation, bioactivity and anti-bacterial activity of produced nanocomposite coatings. The overall results proved that combination of 1 % ZnO and 1% Gr into PLA/PCL/HA membrane could offer a multifunctional platform, a promising alternative for bone disorders and further studies. Given that the Young's modulus of spongy bone is between 0.05 and 0.5 GPa, the optimal matrix is a good option for use in spongy tissue.

ACKNOWLEDGMENT

Thanks to everyone who helped us with this research

Authors' Contribution: Study concept and design, F.D.F,A.R.S, A.A; Acquisition of data, F.D.F; Analysis and interpretation of data, F.D.F, A.R.S, A.A.; Drafting of the manuscript, F.D.F; Critical revision of the manuscript for important intellectual content, A.R.S, A.A; Statistical analysis, F.D.F; Administrative, technical, and material support, A.R.S, F.D.F, A.A; Study supervision, A.R.S, A.A.

Conflict of Interests: It was not declared by the author.

Funding/Support: There is no funding/support.

REFERENCES

[1] Yu X, Tang X, Gohil SV, Laurencin CT. Biomaterials for bone regenerative engineering. Advanced healthcare materials. 2015;4(9):1268-85.

[2] Lim D-J, Sim M, Heo Y, Jun H-W, Park H. Facile method for fabricating uniformly patterned and porous nanofibrous scaffolds for tissue engineering. Macromolecular Research. 2015;23(12):1152-8.

[3] Bigham A, Aghajanian AH, Movahedi M, Sattary M, Rafienia M, Tayebi L. A 3D nanostructured calcium-aluminum-silicate

[DOI: 10.22068/ijmse.2788]

scaffold with hierarchical meso-macroporosity for bone tissue regeneration: Fabrication, sintering behavior, surface modification and in vitro studies. Journal of the European Ceramic Society. 2021;41(1):941-62.

[4] Movahedi M, Ghasemi-Omran V, Torabi S. The effect of different concentrations of TDZ and BA on in vitro regeneration of Iranian cannabis (Cannabis sativa) using cotyledon and epicotyl explants. Journal of Plant Molecular Breeding. 2015;3(2):20-7.

[5] Salehi AOM, Nourbakhsh MS, Rafienia M, Baradaran-Rafii A, Keshel SH. Corneal stromal regeneration by hybrid oriented poly (ε-caprolactone)/lyophilized silk fibroin electrospun scaffold. International Journal of Biological Macromolecules. 2020.

[6] Salehi AOM, Keshel SH, Sefat F, Tayebi L. Use of Polycaprolactone in Corneal Tissue Engineering: A Review. Materials Today Communications. 2021:102402.

[7] Dai T, Tanaka M, Huang Y-Y, Hamblin MR. Chitosan preparations for wounds and burns: antimicrobial and wound-healing effects. Expert review of anti-infective therapy. 2011;9(7):857-79.

[8] Rodríguez-Vázquez M, Vega-Ruiz B, Ramos-Zúñiga R, Saldaña-Koppel DA, Quiñones-Olvera LF. Chitosan and its potential use as a scaffold for tissue engineering in regenerative medicine. BioMed research international. 2015;2015.

[9] Movahedi M, Asefnejad A, Rafienia M, Khorasani MT. Potential of novel electrospun core-shell structured polyurethane/starch (hyaluronic acid) nanofibers for skin tissue engineering: In vitro and in vivo evaluation. International journal of biological macromolecules. 2020;146:627-37.

[10] Hassanajili S, Karami-Pour A, Oryan A, Talaei-Khozani T. Preparation and characterization of PLA / PCL / HA composite scaffolds using indirect 3D printing for bone tissue engineering. Materials Science and Engineering: C. 2019;104:109960.

[11] He H, Yu J, Cao J, E L, Wang D, Zhang H. Biocompatibility and osteogenic capacity of periodontal ligament stem cells on nHAC/PLA and HA/TCP scaffolds. Journal of Biomaterials Science, Polymer Edition. 2011;22(1-3):179-94.

[12] Oryan A, Alidadi S, Bigham-Sadegh A, Meimandi-Parizi A. Chitosan / gelatin / platelet gel enriched by a combination of hydroxyapatite and beta-tricalcium phosphate in healing of a radial bone defect model in rat. International journal of biological macromolecules. 2017;101:630-7.

[13] Hu Y, Zhang Q, You R, Wang L, Li M. The relationship between secondary structure and biodegradation behavior of silk fibroin scaffolds. Advances in Materials Science and Engineering. 2012;2012.

[14] Yin G, Zhao D, Zhang L, Ren Y, Ji S, Tang H. Highly porous 3D PLLA materials composed of nanosheets, fibrous nanosheets, or nanofibrous networks: preparation and the potential application in oil–water separation. Chemical Engineering Journal. 2016;302:1-11.

[15] Takayama T, Todo M, Arakawa K, editors. Characterization of impact fracture behavior of biodegradable PLA / PCL polymer blend. Key Engineering Materials; 2006: Trans Tech Publ.

[16] Movahedi M, Salehi AOM, Moezi D, Yarahmadian R. In vitro and in vivo study of aspirin loaded, electrospun polycaprolactone–maltodextrin membrane for enhanced skin tissue regeneration. International Journal of Polymeric Materials and Polymeric Biomaterials. 2021:1-11.

[17] Bigham A, Salehi AOM, Rafienia M, Salamat MR, Rahmati S, Raucci MG. Zn-substituted Mg2SiO4 nanoparticles-incorporated PCL-silk fibroin composite scaffold: A multifunctional platform towards bone tissue regeneration. Materials Science and Engineering: C. 2021:112242.

[18] Rodenas-Rochina J, Vidaurre A, Cortazár IC, Lebourg M. Effects of hydroxyapatite filler on long-term hydrolytic degradation of PLLA/PCL porous scaffolds. Polymer Degradation and Stability. 2015;119:121-31.

[19] Kiersnowski A, Gutmann JS, Pigłowski J. Influence of organic modifiers on

[DOI: 10.22068/ijmse.2788]

morphology and crystallization of poly (ϵ-caprolactone)/synthetic clay intercalated nanocomposites. Journal of Polymer Science Part B: Polymer Physics. 2007;45(17):2350-67.
[20] Rubner M. Synthetic sea shell. Nature. 2003;423(6943):925-6.
[21] Arun M, Kantheti S, Gaddam RR, Narayan R, Raju K. Surface modification of TiO 2 nanoparticles with 1, 3, 5-triazine based silane coupling agent and its cumulative effect on the properties of polyurethane composite coating. Journal of Polymer Research. 2014;21(12):1-11.
[22] Esmailzadeh H, Sangpour P, Shahraz F, Hejazi J, Khaksar R. Effect of nanocomposite packaging containing ZnO on growth of Bacillus subtilis and Enterobacter aerogenes. Materials Science and Engineering: C. 2016;58:1058-63.
[23] Mallakpour S, Nouruzi N. Effect of modified ZnO nanoparticles with biosafe molecule on the morphology and physiochemical properties of novel polycaprolactone nanocomposites. Polymer. 2016;89:94-101.
[24] Karthikeyan B, Pandiyarajan T, Mangalaraja R. Enhanced blue light emission in transparent ZnO: PVA nanocomposite free standing polymer films. Spectrochimica Acta Part A: Molecular and Biomolecular Spectroscopy. 2016;152:485-90.
[25] Bouzourâa M-B, Naciri AE, Moadhen A, Rinnert H, Guendouz M, Battie Y. Effects of silicon porosity on physical properties of ZnO films. Materials Chemistry and Physics. 2016;175:233-40.
[26] Yang C, Li Q, Tang L, Xin K, Bai A, Yu Y. Synthesis, photocatalytic activity, and photogenerated hydroxyl radicals of monodisperse colloidal ZnO nanospheres. Applied Surface Science. 2015;357:1928-38.
[27] Stanković A, Dimitrijević S, Uskoković D. Influence of size scale and morphology on antibacterial properties of ZnO powders hydrothemally synthesized using different surface stabilizing agents. Colloids and Surfaces B: Biointerfaces. 2013;102:21-8.
[28] Seyedsalehi A, Daneshmandi L, Barajaa M, Riordan J, Laurencin CT. Fabrication and characterization of mechanically competent 3D printed polycaprolactone-reduced graphene oxide scaffolds. Scientific reports. 2020;10(1):1-14.
[29] Wubneh A, Tsekoura EK, Ayranci C, Uludağ H. Current state of fabrication technologies and materials for bone tissue engineering. Acta Biomaterialia. 2018;80:1-30.
[30] Collins MN, Ren G, Young K, Pina S, Reis RL, Oliveira JM. Scaffold fabrication technologies and structure/function properties in bone tissue engineering. Advanced Functional Materials. 2021;31(21):2010609.
[31] Kim HD, Amirthalingam S, Kim SL, Lee SS, Rangasamy J, Hwang NS. Biomimetic materials and fabrication approaches for bone tissue engineering. Advanced healthcare materials. 2017;6(23):1700612.
[32] Shanmugam BK, Rangaraj S, Subramani K, Srinivasan S, Aicher WK, Venkatachalam R. Biomimetic TiO2-chitosan/sodium alginate blended nanocomposite scaffolds for tissue engineering applications. Materials Science and Engineering: C. 2020;110:110710.
[33] Gomes ME, Azevedo HS, Moreira A, Ellä V, Kellomäki M, Reis R. Starch–poly (ε-caprolactone) and starch–poly (lactic acid) fibre-mesh scaffolds for bone tissue engineering applications: structure, mechanical properties and degradation behaviour. Journal of tissue engineering and regenerative medicine. 2008;2(5):243-52.
[34] Ahmed J, Hiremath N, Jacob H. Antimicrobial, rheological, and thermal properties of plasticized polylactide films incorporated with essential oils to Inhibit Staphylococcus aureus and Campylobacter jejuni. Journal of food science. 2016;81(2):E419-E29.
[35] O'Connor JP, Kanjilal D, Teitelbaum M, Lin SS, Cottrell JA. Zinc as a therapeutic agent in bone regeneration. Materials. 2020;13(10):2211.
[36] Shi R, Xue J, He M, Chen D, Zhang L, Tian W. Structure, physical properties, biocompatibility and in vitro/vivo degradation behavior of anti-infective

[DOI: 10.22068/ijmse.2788]

polycaprolactone-based electrospun membranes for guided tissue/bone regeneration. Polymer degradation and stability. 2014;109:293-306.

[37] Etemadi N, Mehdikhani M, Poorazizi E, Rafienia M. Novel bilayer electrospun poly (caprolactone)/silk fibroin/strontium carbonate fibrous nanocomposite membrane for guided bone regeneration. Journal of Applied Polymer Science.50264.

[38] Castro-Mayorga JL, Fabra MJ, Pourrahimi AM, Olsson RT, Lagaron JM. The impact of zinc oxide particle morphology as an antimicrobial and when incorporated in poly (3-hydroxybutyrate-co-3-hydroxyvalerate) films for food packaging and food contact surfaces applications. Food and Bioproducts Processing. 2017;101:32-44.

[39] Murariu M, Doumbia A, Bonnaud L, Dechief AL, Paint Y, Ferreira M. High-performance polylactide/ZnO nanocomposites designed for films and fibers with special end-use properties. Biomacromolecules. 2011;12(5):1762-71.

[40] Deng ZY, Yang JF, Beppu Y, Ando M, Ohji T. Effect of agglomeration on mechanical properties of porous zirconia fabricated by partial sintering. Journal of the American Ceramic Society. 2002;85(8):1961-5.

[41] Ahmed J, Mulla M, Jacob H, Luciano G, Bini T, Almusallam A. Polylactide/poly (ε-caprolactone)/zinc oxide/clove essential oil composite antimicrobial films for scrambled egg packaging. Food Packaging and Shelf Life. 2019;21:100355.

[42] Huang H-Y, Fan F-Y, Shen Y-K, Wang C-H, Huang Y-T, Chern M-J. 3D poly-ε-caprolactone/graphene porous scaffolds for bone tissue engineering. Colloids and Surfaces A: Physicochemical and Engineering Aspects. 2020;606:125393.

[43] Tamjid E, Bagheri R, Vossoughi M, Simchi A. Effect of particle size on the in vitro bioactivity, hydrophilicity and mechanical properties of bioactive glass-reinforced polycaprolactone composites. Materials Science and Engineering: C. 2011;31(7):1526-33.

[44] Moura NKd, Siqueira IA, Machado JPdB, Kido HW, Avanzi IR, Rennó ACM. Production and characterization of porous polymeric membranes of PLA/PCL blends with the addition of hydroxyapatite. Journal of Composites Science. 2019;3(2):45.

[45] Huang X-J, Zeng X-F, Wang J-X, Chen J-F. Transparent dispersions of monodispersed ZnO nanoparticles with ultrahigh content and stability for polymer nanocomposite film with excellent optical properties. Industrial & Engineering Chemistry Research. 2018;57(12):4253-60.

[46] Shankar S, Wang L-F, Rhim J-W. Incorporation of zinc oxide nanoparticles improved the mechanical, water vapor barrier, UV-light barrier, and antibacterial properties of PLA-based nanocomposite films. Materials Science and Engineering: C. 2018;93:289-98.

[47] Rostami F, Tamjid E, Behmanesh M. Drug-eluting PCL/graphene oxide nanocomposite scaffolds for enhanced osteogenic differentiation of mesenchymal stem cells. Materials Science and Engineering: C. 2020;115:111102.

[48] Wu D, Samanta A, Srivastava RK, Hakkarainen M. Nano-graphene oxide functionalized bioactive poly (lactic acid) and poly (ε-caprolactone) nanofibrous scaffolds. Materials. 2018;11(4):566.

[49] 49. Nezakati T, Tan A, Seifalian AM. Enhancing the electrical conductivity of a hybrid POSS–PCL/graphene nanocomposite polymer. Journal of colloid and interface science. 2014;435:145-55.

[50] Sahvieh S, Oryan A, Hassanajili S, Kamali A. Role of bone 1stem cell–seeded 3D polylactic acid/polycaprolactone/hydroxyapatite scaffold on a critical-sized radial bone defect in rat. Cell and Tissue Research. 2021;383(2):735-50.

[51] Al-Wafi R, Mansour S, Ahmed M. Mechanical, microstructural properties and cell adhesion of Sr/Se-hydroxyapatite/graphene/polycaprolactone nanofibers. Journal of Thermoplastic Composite Materials. 2021;34(4):536-56.

[52] Mallakpour S, Nouruzi N. Modification of morphological, mechanical, optical and

[DOI: 10.22068/ijmse.2788]

thermal properties in polycaprolactone-based nanocomposites by the incorporation of diacid-modified ZnO nanoparticles. Journal of Materials Science. 2016;51(13):6400-10.

[53] Shrestha BK, Shrestha S, Tiwari AP, Kim J-I, Ko SW, Kim H-J. Bio-inspired hybrid scaffold of zinc oxide-functionalized multi-wall carbon nanotubes reinforced polyurethane nanofibers for bone tissue engineering. Materials & Design. 2017;133:69-81.

[54] Rajitha K, Mohana KN. Application of modified graphene oxide–Polycaprolactone nanocomposite coating for corrosion control of mild steel in saline medium. Materials Chemistry and Physics. 2020;241:122050.

[55] Toloue EB, Karbasi S, Salehi H, Rafienia M. Potential of an electrospun composite scaffold of poly (3-hydroxybutyrate)-chitosan/alumina nanowires in bone tissue engineering applications. Materials Science and Engineering: C. 2019;99:1075-91.

[56] Rafienia M, Bigham A, Saudi A, Rahmati S. Gehlenite nanobioceramic: Sol-gel synthesis, characterization, and in vitro assessment of its bioactivity. Materials Letters. 2018;225:89-92.

[57] Zadpoor AA. Relationship between in vitro apatite-forming ability measured using simulated body fluid and in vivo bioactivity of biomaterials. Materials Science and Engineering: C. 2014;35:134-43.

[58] Ghorghi M, Rafienia M, Nasirian V, Bitaraf FS, Gharravi AM, Zarrabi A. Electrospun captopril-loaded PCL-carbon quantum dots nanocomposite scaffold: Fabrication, characterization, and in vitro studies. Polymers for Advanced Technologies. 2020;31(12):3302-15.

[59] Bigham A, Foroughi F, Ghomi ER, Rafienia M, Neisiany RE, Ramakrishna S. The journey of multifunctional bone scaffolds fabricated from traditional toward modern techniques. Bio-Design and Manufacturing. 2020:1-26.

[60] Brown A, Zaky S, Ray Jr H, Sfeir C. Porous magnesium/PLGA composite scaffolds for enhanced bone regeneration following tooth extraction. Acta biomaterialia. 2015;11:543-53.

[61] Kim K-J, Choi S, Cho YS, Yang S-J, Cho Y-S, Kim KK. Magnesium ions enhance infiltration of osteoblasts in scaffolds via increasing cell motility. Journal of Materials Science: Materials in Medicine. 2017;28(6):96.

[62] Bigham A, Foroughi F, Motamedi M, Rafienia M. Multifunctional nanoporous magnetic zinc silicate-ZnFe2O4 core-shell composite for bone tissue engineering applications. Ceramics International. 2018;44(10):11798-806.

[63] Shankar S, Jaiswal L, Selvakannan P, Ham K, Rhim J. Gelatin-based dissolvable antibacterial films reinforced with metallic nanoparticles. RSC advances. 2016;6(71):67340-52.

[64] Banthia S, Hazra C, Sen R, Das S, Das K. Electrodeposited functionally graded coating inhibits Gram-positive and Gram-negative bacteria by a lipid peroxidation mediated membrane damage mechanism. Materials Science and Engineering: C. 2019;102:623-33.

[65] Xie Y, He Y, Irwin PL, Jin T, Shi X. Antibacterial activity and mechanism of action of zinc oxide nanoparticles against Campylobacter jejuni. Applied and environmental microbiology. 2011; 77(7) : 2325.

[66] Wang Y-W, Cao A, Jiang Y, Zhang X, Liu J-H, Liu Y, et al. Superior antibacterial activity of zinc oxide/graphene oxide composites originating from high zinc concentration localized around bacteria. ACS applied materials & interfaces. 2014;6(4):2791-8.

[67] El-Shafai N, El-Khouly ME, El-Kemary M, Ramadan M, Eldesoukey I, Masoud M. Graphene oxide decorated with zinc oxide nanoflower, silver and titanium dioxide nanoparticles: fabrication, characterization, DNA interaction, and antibacterial activity. RSC advances. 2019;9(7):3704-14.

[68] Liu J, Wang Y, Ma J, Peng Y, Wang A. A review on bidirectional analogies between the photocatalysis and antibacterial properties of ZnO. Journal of Alloys and Compounds. 2019;783:898-918.

[DOI: 10.22068/ijmse.2788]

[69] Thangavel S, Krishnamoorthy K, Krishnaswamy V, Raju N, Kim SJ, Venugopal G. Graphdiyne–ZnO nanohybrids as an advanced photocatalytic material. The Journal of Physical Chemistry C. 2015;119(38):22057-65.

[70] Fang R, Zhang E. Electrospun PCL/PLA/HA Based Nanofibers as Scaffold for Osteoblast- Like Cells. Nanoscience and Nanotechnology 2010; 7747–7751.

[DOI: 10.22068/ijmse.2788]